

Single Spin Asymmetries of Inclusive Hadrons Produced in Electron Scattering from a Transversely Polarized ^3He Target

K. Allada,^{1,2,*} Y.X. Zhao,³ K. Aniol,⁴ J.R.M. Annand,⁵ T. Averett,⁶ F. Benmokhtar,⁷ W. Bertozzi,¹ P.C. Bradshaw,⁶ P. Bosted,² A. Camsonne,² M. Canan,⁸ G.D. Cates,⁹ C. Chen,¹⁰ J.-P. Chen,² W. Chen,¹¹ K. Chirapatpimol,⁹ E. Chudakov,² E. Cisbani,^{12,13} J.C. Cornejo,⁴ F. Cusanno,¹⁴ M. Dalton,⁹ W. Deconinck,¹ C.W. de Jager,² R. De Leo,¹⁵ X. Deng,⁹ A. Deur,² H. Ding,⁹ P. A. M. Dolph,⁹ C. Dutta,¹⁶ D. Dutta,¹⁷ L. El Fassi,¹⁸ S. Frullani,^{14,13} H. Gao,¹¹ F. Garibaldi,^{14,13} D. Gaskell,² S. Gilad,¹ R. Gilman,^{2,18} O. Glamazdin,¹⁹ S. Golge,⁸ L. Guo,²⁰ D. Hamilton,⁵ O. Hansen,² D.W. Higinbotham,² T. Holmstrom,²¹ J. Huang,^{1,20} M. Huang,¹¹ H. F Ibrahim,²² M. Iodice,²³ X. Jiang,^{18,20} G. Jin,⁹ M.K. Jones,² J. Katich,⁶ A. Kelleher,⁶ W. Kim,²⁴ A. Kolarkar,¹⁶ W. Korsch,¹⁶ J.J. LeRose,² X. Li,²⁵ Y. Li,²⁵ R. Lindgren,⁹ N. Liyanage,⁹ E. Long,²⁶ H.-J. Lu,³ D.J. Margaziotis,⁴ P. Markowitz,²⁷ S. Marrone,¹⁵ D. McNulty,²⁸ Z.-E. Meziani,²⁹ R. Michaels,² B. Moffit,^{1,2} C. Muñoz Camacho,³⁰ S. Nanda,² A. Narayan,¹⁷ V. Nelyubin,⁹ B. Norum,⁹ Y. Oh,³¹ M. Osipenko,³² D. Parno,⁷ J.-C. Peng,³³ S. K. Phillips,³⁴ M. Posik,²⁹ A. J. R. Puckett,^{1,20} X. Qian,³⁵ Y. Qiang,^{11,2} A. Rakhman,³⁶ R. Ransome,¹⁸ S. Riordan,⁹ A. Saha,^{2,†} B. Sawatzky,^{29,2} E. Schulte,¹⁸ A. Shahinyan,³⁷ M. H. Shabestari,⁹ S. Širca,³⁸ S. Stepanyan,³⁹ R. Subedi,⁹ V. Sulkosky,^{1,2} L.-G. Tang,¹⁰ A. Tobias,⁹ G. M. Urciuoli,¹⁴ I. Vilardi,¹⁵ K. Wang,⁹ Y. Wang,³³ B. Wojtsekhowski,² X. Yan,³ H. Yao,²⁹ Y. Ye,³ Z. Ye,¹⁰ L. Yuan,¹⁰ X. Zhan,¹ Y. Zhang,⁴⁰ Y.-W. Zhang,⁴⁰ B. Zhao,⁶ X. Zheng,⁹ L. Zhu,^{33,10} X. Zhu,¹¹ and X. Zong¹¹

(The Jefferson Lab Hall A Collaboration)

¹Massachusetts Institute of Technology, Cambridge, MA 02139

²Thomas Jefferson National Accelerator Facility, Newport News, VA 23606

³University of Science and Technology of China, Hefei 230026, Peoples Republic of China

⁴California State University, Los Angeles, Los Angeles, CA 90032

⁵University of Glasgow, Glasgow G12 8QQ, Scotland, United Kingdom

⁶College of William and Mary, Williamsburg, VA 23187

⁷Carnegie Mellon University, Pittsburgh, PA 15213

⁸Old Dominion University, Norfolk, VA 23529

⁹University of Virginia, Charlottesville, VA 22904

¹⁰Hampton University, Hampton, VA 23187

¹¹Duke University, Durham, NC 27708

¹²INFN, Sezione di Roma, I-00185 Rome, Italy

¹³Istituto Superiore di Sanità, I-00161 Rome, Italy

¹⁴INFN, Sezione di Roma, I-00161 Rome, Italy

¹⁵INFN, Sezione di Bari and University of Bari, I-70126 Bari, Italy

¹⁶University of Kentucky, Lexington, KY 40506

¹⁷Mississippi State University, MS 39762

¹⁸Rutgers, The State University of New Jersey, Piscataway, NJ 08855

¹⁹Kharkov Institute of Physics and Technology, Kharkov 61108, Ukraine

²⁰Los Alamos National Laboratory, Los Alamos, NM 87545

²¹Longwood University, Farmville, VA 23909

²²Cairo University, Giza 12613, Egypt

²³INFN, Sezione di Roma Tre, I-00146 Rome, Italy

²⁴Kyungpook National University, Taegu 702-701, Republic of Korea

²⁵China Institute of Atomic Energy, Beijing, Peoples Republic of China

²⁶Kent State University, Kent, OH 44242

²⁷Florida International University, Miami, FL 33199

²⁸University of Massachusetts, Amherst, MA 01003

²⁹Temple University, Philadelphia, PA 19122

³⁰Université Blaise Pascal/IN2P3, F-63177 Aubière, France

³¹Seoul National University, Seoul, South Korea

³²INFN, Sezione di Genova, I-16146 Genova, Italy

³³University of Illinois, Urbana-Champaign, IL 61801

³⁴University of New Hampshire, Durham, NH 03824

³⁵Physics Department, Brookhaven National Laboratory, Upton, NY

³⁶Syracuse University, Syracuse, NY 13244

³⁷Yerevan Physics Institute, Yerevan 375036, Armenia

³⁸University of Ljubljana, SI-1000 Ljubljana, Slovenia

³⁹Kyungpook National University, Taegu City, South Korea

⁴⁰Lanzhou University, Lanzhou 730000, Gansu, Peoples Republic of China

(Dated: March 20, 2014)

We report the first measurement of target single-spin asymmetries (A_N) in the inclusive hadron production reaction, $e + {}^3\text{He}^\uparrow \rightarrow h + X$, using a transversely polarized ${}^3\text{He}$ target. The experiment was conducted at Jefferson Lab in Hall A using a 5.9-GeV electron beam. Three types of hadrons (π^\pm , K^\pm and proton) were detected in the transverse hadron momentum range $0.54 < p_T < 0.74$ GeV/c. The range of x_F for pions was $-0.29 < x_F < -0.23$ and for kaons $-0.25 < x_F < -0.18$. The observed asymmetry strongly depends on the type of hadron. A positive asymmetry is observed for π^+ and K^+ . A negative asymmetry is observed for π^- . The magnitudes of the asymmetries follow $|A^{\pi^-}| < |A^{\pi^+}| < |A^{K^+}|$. The K^- and proton asymmetries are consistent with zero within the experimental uncertainties. The π^+ and π^- asymmetries measured for the ${}^3\text{He}$ target and extracted for neutrons are opposite in sign with a small increase observed as a function of p_T .

PACS numbers: 14.20.Dh, 25.30.Fj, 25.30.Rw, 24.85.+p

The study of the transverse single spin asymmetries (TSSAs) is one of the most active areas of research in modern hadronic physics. TSSA is an important tool to advance our understanding of the nucleon spin, to reveal the role of the quark orbital angular momentum (OAM), and to access the three-dimensional structure of the nucleon in momentum space [1]. Current research on TSSA focuses on the polarized proton-proton (pp^\uparrow) and lepton-nucleon (lN^\uparrow) reaction channels.

An early observation of large left-right SSAs (A_N) in the $pp^\uparrow \rightarrow \pi^\pm X$ reaction by the Fermilab E704 experiment at $\sqrt{s}=19.4$ GeV [2, 3] revealed a strong dependence on the hadron type. In the center-of-mass frame of the polarized pp^\uparrow collision, viewed along the momentum direction of the polarized proton, π^+ favors the left side of the spin vector, whereas π^- favors the right side of the spin vector. More recently, such non-vanishing TSSAs were observed for π^\pm and K^\pm at $\sqrt{s}=62.4$ GeV by BRAHMS [4], and for neutral pions at $\sqrt{s}=200$ GeV by the STAR experiment at RHIC [5]. Although TSSAs have been observed in pp^\uparrow reactions for more than two decades, measurement in semi-inclusive deep inelastic scattering (SIDIS) is regarded as one of the cleanest ways to understand them at the partonic level. TSSAs have been measured in the SIDIS reaction ($lp^\uparrow \rightarrow l'hX$) by HERMES [6–9] with a polarized proton target, and by COMPASS [10–13] using polarized proton and deuteron targets. Recently, they have been measured at Jefferson Lab in Hall A using a polarized ${}^3\text{He}$ target [14, 15].

The origin of TSSAs is currently interpreted using two theoretical approaches [16]. The first approach is based on the transverse-momentum-dependent distribution and fragmentation functions (TMDs) in the framework of the TMD factorization, and is mostly used to explain TSSAs in the SIDIS process. There are two reaction mechanisms: the Collins effect [17] and the Sivers effect [18]. In the Collins effect, the TSSA is generated by the transversity distribution, which represents the probability of finding a transversely polarized parton inside a transversely polarized nucleon, and the Collins fragmentation function, which correlates the transverse polarization of the

quark with the transverse momentum of the outgoing hadron (p_T). In the Sivers effect, the TSSA is generated by the Sivers distribution function, which correlates the quark's transverse momentum and the nucleon's spin, and is sensitive to the quark OAM. More specifically, the observed asymmetry due to the Sivers function arises from the final-state interaction between the struck quark and the nucleon remnant in SIDIS. On the other hand, the Sivers function in the Drell-Yan process is expected to arise from the initial-state interactions [19]. Taking gauge links into consideration, the Sivers distribution is predicted to be process dependent in the sense that it differs in sign between SIDIS and Drell-Yan processes [19, 20]. Furthermore, in models such as the di-quark model [21], one can connect the Sivers distribution for each quark to its contribution to the anomalous magnetic moment of the nucleon.

The second approach is based on the twist-3 collinear factorization [22–25], where the SSAs are interpreted in terms of higher-twist quark-gluon correlations, and is mainly used to explain the TSSAs in the $pp^\uparrow \rightarrow hX$ channel. It was also shown that the TMD factorization and twist-3 methods are related [26–28]. However, the Sivers function extracted from pp^\uparrow data with the twist-3 approach is shown to have a “sign mismatch” when compared to the Sivers function extracted from SIDIS data. The sign mismatch indicates a potential inconsistency in the current theoretical formalism [29], and needs to be further investigated. In order to understand the underlying mechanism producing TSSA it is crucial to study additional reaction channels [16, 30].

In this letter, we study TSSA from one of the experimentally least explored reactions, inclusive hadron production using a lepton beam on a transversely polarized nucleon ($lN^\uparrow \rightarrow hX$) [16, 31]. An early study of this process was done by Anselmino *et al.*, under the assumption that the underlying mechanism that generates TSSA is either Collins or Sivers effect [31]. More recently, this study was re-evaluated using newly available SIDIS data on Sivers and Collins moments assuming that the TMD factorization is valid in $lp^\uparrow \rightarrow \pi^\pm X$ processes at large p_T values. Due to the presence of only one hard scale in this process, estimation of the asymmetries is generally done at large p_T values (typically >1 GeV/c). They

* Corresponding author: kalyan@jlab.org

† Deceased

predicted asymmetries between 5-10% for $\sqrt{s} \simeq 4.9$ GeV, $p_T = 1.5$ GeV/c, and $x_F \leq 0.1$ with a contribution from the Sivers mechanism to A_N , whereas the contribution from the Collins mechanism was negligible [16].

Non-zero SSAs were also estimated based on the twist-3 distribution and fragmentation functions in the framework of collinear factorization [30, 32, 33], and in the SIDIS process by integrating over the scattered electron's azimuthal angle [34]. These studies of TSSAs in the $lp^\uparrow \rightarrow \pi^\pm X$ process are performed under the assumption of a SIDIS reaction, in which hard scattering occurs between a virtual photon and a quark. However, since the process is dominated by the cross-section at Q^2 near zero, it was also pointed out that the $lp^\uparrow \rightarrow \pi^\pm X$ process will have significant contributions from soft processes, such as vector meson dominance, especially at lower p_T values [35]. Experimental data for TSSA in this process have recently been reported by the HERMES Collaboration using e^-/e^+ beams on a transversely polarized hydrogen target [9].

We report the first measurement of target single-spin asymmetries (A_N) in inclusive hadron (π^\pm , K^\pm , and proton) production at fixed-target e+N center-of-mass energy $\sqrt{s} = 3.45$ GeV, using an unpolarized electron beam and a transversely polarized ^3He target as an effective polarized neutron target. The kinematical variables for this process are: $x_F = 2p^{CM}/\sqrt{s}$, where p^{CM} is the momentum of the outgoing hadron along the polarized nucleon's momentum direction in the e+N center-of-mass frame, and $p_T = \sqrt{p_x^2 + p_y^2}$, the transverse momentum of the outgoing hadron. The kinematical configuration in the laboratory coordinate system is shown in Fig 1. The target spin “up” (\uparrow) was defined to be along the $+\hat{y}$

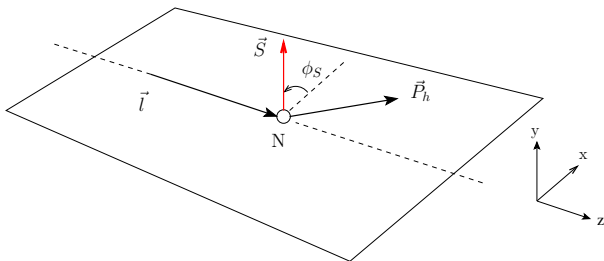


FIG. 1. (Color online) Kinematical configuration in the laboratory coordinate system for the $lN^\uparrow \rightarrow hX$ process. \vec{P}_h represents the momentum direction of the produced hadron, and \vec{S} is the spin vector of the nucleon. The polarized nucleon's momentum is along the $-z$ direction in the e+N center-of-mass frame

direction, parallel to the vector $\vec{l} \times \vec{P}_h$ ($\phi_S = 90^\circ$), where \vec{l} and \vec{P}_h are the momentum vectors of the incoming beam and outgoing hadron, respectively.

The target SSA is defined as [16],

$$A_{UT}(x_F, p_T) = \frac{1}{P} \frac{d\sigma^\uparrow - d\sigma^\downarrow}{d\sigma^\uparrow + d\sigma^\downarrow} \sin\phi_S = A_N \sin\phi_S, \quad (1)$$

where $d\sigma^{\uparrow(\downarrow)}$ is the differential cross-section in the target “up” (“down”) state, and P is the target polarization. The spin-dependent part of the cross-section is proportional to the term $\vec{S} \cdot (\vec{l} \times \vec{P}_h)$, which gives rise to a $\sin(\phi_S)$ modulation in the definition of the asymmetry. This term makes A_N parity-conserving, but T-odd under “naïve” time reversal, in which the initial and final states do not interchange. Note that the sign of A_N in the laboratory coordinate system of this experiment (Eq. 1) differ by a factor -1 from the definition in the phenomenological study of this process in [16], where the authors used the center-of-mass coordinate system with the lepton moving in the $-\hat{z}$ direction.

The data were collected using a singles trigger during the E06-010 experiment in Hall A at Jefferson Lab [36]. A beam energy of 5.9 GeV was provided by the CEBAF accelerator with an average current of 12 μA . The produced hadrons were detected in a high-resolution spectrometer (HRS) [37] at a central angle of 16° on beam left side. Positively and negatively charged particles were detected separately by changing the magnet polarity of the HRS. The central momentum of the HRS was fixed at 2.35 GeV/c, with a momentum acceptance of $\pm 4.5\%$ and solid angle of 6 msr. The average transverse momentum of the detected hadrons ($\langle p_T \rangle$) was 0.64 GeV/c. We note that if the pions are produced through virtual or real-photon exchange ($\gamma^* + N$ or $\gamma + N$), the minimum photon energy is $E_\gamma \geq 2.6$ GeV, corresponding to an invariant mass of $W \geq 2.4$ GeV for the $\gamma + N$ system, well above the region of nucleon resonances.

The data from the two helicity states from the polarized electron beam were summed over to achieve an unpolarized beam. The residual helicity-sorted beam-charge difference was less than 100 ppm in a typical run. The target spin direction was automatically reversed ($\phi_S = \pm 90^\circ$) at a rate of once every 20 minutes, which allowed control of the combined systematic uncertainty due to luminosity fluctuations and time dependence to below 50 ppm in this experiment.

Polarized ^3He targets have often been used as an effective polarized neutron targets, because in the ground state of the ^3He nuclear wavefunction (dominated by the S-state) the two proton spins are opposite to each other, and the nuclear spin is carried by the remaining neutron [38]. The polarized target used in this measurement was a 40-cm long glass cell filled with ~ 8 atm of ^3He gas and a small amount (~ 0.13 atm) of N_2 gas to reduce depolarizing effects [37]. The radiation lengths of the materials up to the center of the ^3He target were: Be window (0.072%), ^4He gas (0.004%), glass window (0.142%), and ^3He gas (0.046%). The target was polarized via hybrid spin-exchange optical pumping of a mixture of Rb-K [39]. The ^3He polarization was measured every 20 minutes during the spin-reversal using Nuclear Magnetic Resonance (NMR). The NMR signal was calibrated with Electron Paramagnetic Resonance (EPR) measurements and a known NMR signal obtained from an identical water cell. The average in-beam polarization

of the target was $(55.4 \pm 2.8)\%$.

The HRS detector package consisted of four separate detectors for particle identification: (i) a light-gas threshold Čerenkov for electron identification, (ii) a two-layer electromagnetic calorimeter for electron-hadron separation, (iii) a threshold aerogel Čerenkov detector for pion identification, and (iv) a ring imaging Čerenkov (RICH) detector for π^\pm , K^\pm , and proton identification. The electron and positron background were suppressed with a rejection factor of $10^4:1$. After all the particle identification cuts the contamination due to leptons was negligible in the hadron sample. The pion sample had a contamination of $<1\%$ due to other hadrons. Kaons were identified using the RICH detector, in combination with a veto from the aerogel counter, to suppress the large pion background. To further improve the purity of the kaon sample, a χ^2 probability distribution was constructed based on the reconstructed Čerenkov ring angle and the expected Čerenkov angle in the RICH detector for a known particle momentum [40]. A cut on this distribution effectively suppresses the background events due to misidentified particles. The contamination of the kaon sample from other hadrons was estimated to be $\sim 3\%$ (proton) and $\sim 2\%$ (π^+) for positive kaons, and $\sim 2\%$ (π^-) for negative kaons. Protons were identified using the same method that was used for charged kaons, producing a very clean sample with estimated background $<1\%$.

The raw ^3He target single-spin asymmetry (A_N) was obtained using the normalized yields in target spin up/down ($\phi_S = \pm 90^\circ$) states, as shown in Eq. 1. The yield in each spin state is normalized with the accumulated beam charge and livetime of the data acquisition system in that state. The dilution of the measured ^3He asymmetries due to the presence of a small amount of N_2 gas in the target cell was corrected using the factor,

$$f_{\text{N}_2} \equiv \frac{\rho_{\text{N}_2} \sigma_{\text{N}_2}}{\rho_{^3\text{He}} \sigma_{^3\text{He}} + \rho_{\text{N}_2} \sigma_{\text{N}_2}}, \quad (2)$$

where ρ is the density of the gas in the cell and σ is the unpolarized inclusive hadron cross-section. The unpolarized N_2 and ^3He cross-sections were obtained from the data taken during the experiment using reference cells filled with pure N_2 and ^3He gas. The f_{N_2} was extracted separately for all hadrons and was about $\sim 10\%$ in each case.

The overall systematic uncertainty in this measurement was small due to frequent target spin flips. The false asymmetry due to luminosity fluctuations was less than 0.04% and was confirmed by measuring the target SSA in inclusive (e, e') DIS reaction for in-plane transverse target ($\phi_S = 0^\circ, 180^\circ$). This configuration was achieved by rotating the target spin by 90° while keeping all other conditions the same. This type of asymmetry vanishes under parity conservation, assuming one-photon exchange. In addition, the inclusive pion asymmetry was measured to be zero with a precision of 0.05% in the same configuration ($\phi_S = 0^\circ, 180^\circ$). This asymmetry is expected to vanish due to $\sin(\phi_S)$ moment.

There were two additional sources of systematic uncertainty associated with the RICH detector for kaons and protons. The first one was from a cut on the number of hits in the RICH detector. The relative change in asymmetry under variation of the cut threshold was assigned as a systematic uncertainty. For K^\pm it was $<14\%$ and for protons it was $<3\%$, relative to the statistical uncertainty. The second source was local fluctuations in the kaon and proton yield arising from detector inefficiencies in certain periods of the data-taking. The systematic uncertainty was estimated using the change in the asymmetry obtained in the periods with and without these fluctuations, and was estimated to be $<2\%$, $<6\%$, and $<1\%$, relative to the statistical uncertainty, for K^+ , K^- and protons, respectively. Systematic uncertainties due to the target density fluctuations, vertex cuts, DAQ livetime, and HRS single-track events were negligible.

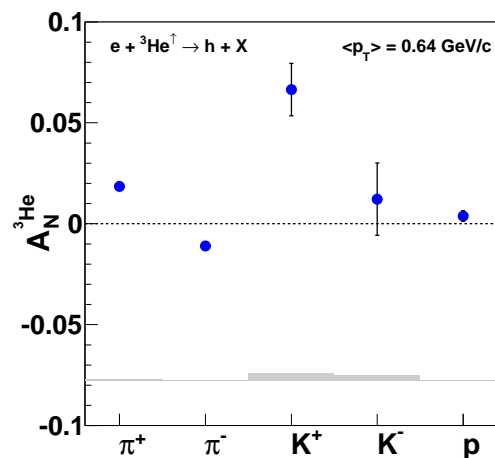


FIG. 2. (Color online) Inclusive SSA results on a ^3He target for π^\pm , K^\pm and protons in the vertical target spin configuration ($\phi_S = \pm 90^\circ$). The error bars on the points represents the statistical uncertainty. The grey band shows the magnitude of the overall systematic uncertainty for each hadron channel.

The final ^3He asymmetry results are shown for different hadron species in Fig. 2. These results include a small correction due to particle contamination for each hadron species. In Fig. 2 the data were integrated in p_T and x_F (see Table I). The error bars represents the statistical uncertainty. The systematic uncertainties are shown as a solid band. The measured A_N for π^+ ($\sim 2\%$) and K^+ ($\sim 6\%$) are positive, and opposite in sign to that of π^- ($\sim 1\%$). In addition, the magnitudes of these asymmetries follow $|A^{\pi^-}| < |A^{\pi^+}| < |A^{K^+}|$. The measured A_N for K^- and protons was found to be small and consistent with zero. We note that the majority of the detected protons originate through a knock-out reaction from the ^3He nucleus, whereas mesons are produced either through fragmentation process or in a photoproduction reaction. The SSAs for charged pions as a function of p_T for a ^3He target are shown in Fig. 3. The asymmetry grows as a function of p_T and plateaus around $p_T \simeq 0.63 \text{ GeV}/c$.

Hadron	$\langle x_F \rangle$	$\langle p_T \rangle$ (GeV/c)	$A_N^{3\text{He}} \pm \text{Stat.} \pm \text{Sys.}$
π^+	-0.262	0.64	$0.0185 \pm 0.0007 \pm 0.0009$
π^-	-0.262	0.64	$-0.0109 \pm 0.0005 \pm 0.0005$
K^+	-0.215	0.64	$0.0665 \pm 0.0130 \pm 0.0038$
K^-	-0.215	0.64	$0.0122 \pm 0.0179 \pm 0.0027$
p	-0.087	0.64	$0.0038 \pm 0.0026 \pm 0.0002$

TABLE I. Central kinematics for three types of hadrons along with the A_N results for a ${}^3\text{He}$ target. A negative x_F indicates that the produced hadron is moving backwards with respect to the nucleon momentum direction in the center-of-mass frame of the e+N system.

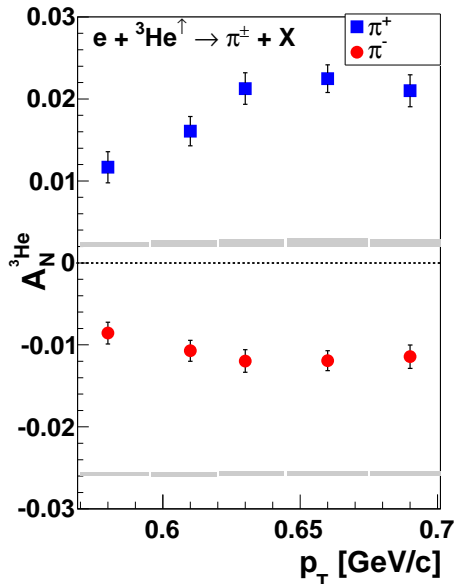


FIG. 3. (Color online) A_N results on a ${}^3\text{He}$ target for the π^\pm channel as a function of p_T . The solid band on the bottom of each panel shows the magnitude of the systematic uncertainty for each momentum bin.

We extracted A_N on neutron from the measured ${}^3\text{He}$ asymmetry using the effective polarization approach, previously used for both inclusive and semi-inclusive DIS processes [38, 41]. Using this method, A_N for the neutron can be obtained from ${}^3\text{He}$ results using the relation,

$$A_N^{3\text{He}} = P_n(1 - f_p)A_N^n + P_p f_p A_N^p, \quad (3)$$

where $A_N^{3\text{He}}$ is the measured ${}^3\text{He}$ asymmetry. $P_n = 0.86^{+0.036}_{-0.02}$ and $P_p = -0.028^{+0.009}_{-0.004}$ are the effective polarization of the neutron and proton, respectively. Hence, the contribution of proton polarization ($\simeq 2.8\%$) to $A_N^{3\text{He}}$ is relatively small. The factor, $f_p = \frac{2\sigma_p}{\sigma_{3\text{He}}}$, in ${}^3\text{He}$ was measured directly in this experiment using the yields obtained from unpolarized hydrogen and ${}^3\text{He}$ targets. The average proton dilution ($1 - f_p$) for π^+ was 0.156 ± 0.007 and for π^- it was 0.268 ± 0.005 . The SSA from a polarized proton target (A_N^p) was assumed to be no more than

$\pm 5\%$ at $p_T \simeq 0.64$ GeV/c, which is consistent with the HERMES data on A_N^p [9].

The final results for A_N^n for charged pions on an effective neutron target are shown in Fig. 4. The extracted A_N^n is below 20% for both π^+ and π^- , with the asymmetry amplitude for π^+ being larger than those for π^- . The A_N^n for both π^+ and π^- increase up to $p_T \simeq 0.63$ GeV/c, before it plateaus. Currently there are no theoretical estimates for A_N at $\sqrt{s} = 3.45$ GeV and $\langle p_T \rangle \sim 0.64$ GeV/c for a neutron target. The existing predictions were done for a proton target at $p_T = 1.5$ GeV/c and $\sqrt{s} \simeq 4.9$ GeV [16]. However, the sign of A_N for π^\pm in our experiment is consistent with the existing predictions dominated by the Sivers effect, assuming $p \leftrightarrow n$ and $\pi^+ \leftrightarrow \pi^-$.

$\langle p_T \rangle$ (GeV/c)	$A_N^n(\pi^+) \pm \text{Stat.} \pm \text{Sys.}$	$A_N^n(\pi^-) \pm \text{Stat.} \pm \text{Sys.}$	R_{π^+/π^-}
0.58	$0.109 \pm 0.016 \pm 0.007$	$-0.044 \pm 0.006 \pm 0.003$	-2.5 ± 0.5
0.61	$0.125 \pm 0.013 \pm 0.008$	$-0.051 \pm 0.005 \pm 0.003$	-2.5 ± 0.4
0.63	$0.166 \pm 0.014 \pm 0.010$	$-0.055 \pm 0.006 \pm 0.004$	-3.0 ± 0.5
0.66	$0.169 \pm 0.012 \pm 0.010$	$-0.056 \pm 0.005 \pm 0.004$	-3.0 ± 0.4
0.69	$0.160 \pm 0.014 \pm 0.010$	$-0.053 \pm 0.006 \pm 0.003$	-3.0 ± 0.5

TABLE II. The extracted neutron A_N^n results for π^+ and π^- along with their ratio R_{π^+/π^-} in five different $\langle p_T \rangle$ bins.

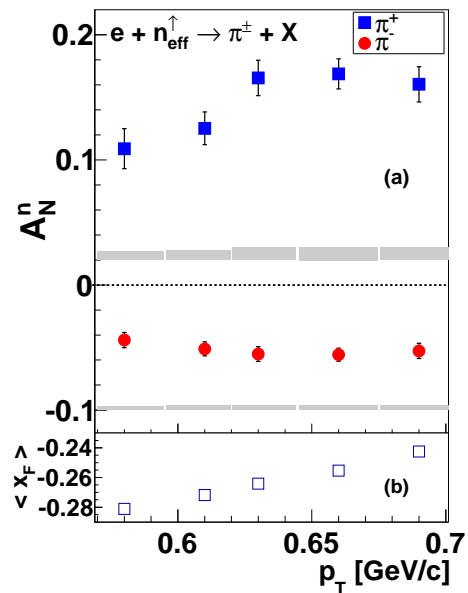


FIG. 4. (Color online) (a) A_N^n results on a neutron target extracted from the measured ${}^3\text{He}$ asymmetries. The solid band on the bottom of each panel shows the magnitude of the systematic uncertainty for each momentum bin. The lower plot (b) is the x_F and p_T correlation in this measurement.

We can compare the observed behavior of our data with existing TSSAs in both proton-proton (pp^\uparrow) and lepton-nucleon (lN^\uparrow) reaction channels. Our results show that in the center-of-mass frame of the polarized neutron-

electron collision, viewed along the direction of the neutron's momentum, π^+ favors the right side of the spin vector, whereas π^- favors the left side of the spin vector. Assuming isospin symmetry, this behavior is the same as that observed in $pp^\uparrow \rightarrow hX$ for the E704 [2, 3] and BRAHMS [4] experiments. In addition, this behavior is also the same as the Collins asymmetry for π^\pm , and the Sivers asymmetry for π^+ observed in SIDIS [6–8, 12–14]. The A_N^n for π^+ is about $\sim 15\%$ at $\langle p_T \rangle = 0.64$ GeV/c, which is larger than that for HERMES proton data for π^+ ($\sim 5\%$ at $\langle p_T \rangle = 0.68$ GeV/c) [9]. Similarly, we observed large A_N^n for π^- ($\sim 5\%$) compared to that for HERMES proton data ($<1\%$) [9]. Furthermore, we observed a large and positive amplitude for the K^+ asymmetry compared to K^- asymmetry on ^3He , a similar feature observed in $lp^\uparrow \rightarrow hX$ reaction on proton target [9], and also the Sivers amplitude for kaons in the SIDIS reaction at HERMES [7].

In summary, we have reported the first measurement of SSAs in the inclusive hadron production reaction using unpolarized electrons on a transversely polarized ^3He target at $\langle p_T \rangle = 0.64$ GeV/c. Clear non-zero asymmetries were observed for charged pions and positive kaons,

showing a similar feature of flavor dependence to that observed in the Sivers asymmetry in SIDIS, and in A_N in pp^\uparrow collisions. Currently there are no estimates or theoretical interpretations of these asymmetries at the relatively low p_T of 0.64 GeV/c used for this measurement. We hope that the results presented here will stimulate new theoretical and experimental efforts to pin-point the exact origin of the observed SSAs. Future experiments at Jefferson Lab [42, 43], after the 12-GeV upgrade, will extend this measurement to higher values of p_T on both proton and ^3He targets, and will provide precision data for future theoretical studies. Moreover, if these non-zero asymmetries survive at high energy kinematics then they can be used as monitors of transverse target polarization in a fixed target experiment, or local transverse polarization of the ^3He beam at a future Electron-Ion-Collider.

We acknowledge the outstanding support of the JLab Hall A staff and the Accelerator Division in accomplishing this experiment. This work was supported in part by the U. S. National Science Foundation, and by Department of Energy (DOE) contract number DE-AC05-06OR23177, under which the Jefferson Science Associates operates the Thomas Jefferson National Accelerator Facility.

-
- [1] V. Barone *et al.*, *Prog. in Part. and Nucl. Phys.* **65**, 267 (2010).
- [2] D. Adams *et al.*, *Phys. Lett. B* **264**, 462 (1991).
- [3] D. Adams *et al.*, *Phys. Lett. B* **261**, 201 (1991).
- [4] I. Arsene *et al.*, *Phys. Rev. Lett.* **101**, 042001 (2008).
- [5] B. I. Abelev *et al.*, *Phys. Rev. Lett.* **101**, 222001 (2008).
- [6] A. Airapetian *et al.*, *Phys. Rev. Lett.* **94**, 012002 (2005).
- [7] A. Airapetian *et al.*, *Phys. Rev. Lett.* **103**, 152002 (2009).
- [8] A. Airapetian *et al.*, *Phys. Lett. B* **693**, 11 (2010).
- [9] A. Airapetian *et al.*, *Phys. Lett. B* **728**, 183 (2014).
- [10] M. G. Alekseev *et al.*, *Phys. Lett. B* **692**, 240 (2010).
- [11] M. Alekseev *et al.*, *Phys. Lett. B* **673**, 127 (2009).
- [12] C. Adolph *et al.*, *Phys. Lett. B* **717**, 376 (2012).
- [13] C. Adolph *et al.*, *Phys. Lett. B* **717**, 383 (2012).
- [14] X. Qian *et al.*, *Phys. Rev. Lett.* **107**, 072003 (2011).
- [15] J. Huang *et al.*, *Phys. Rev. Lett.* **108**, 052001 (2012).
- [16] M. Anselmino *et al.*, *Phys. Rev. D* **81**, 034007 (2010).
- [17] J. Collins, *Nuclear Physics B* **396**, 161 (1993).
- [18] D. Sivers, *Phys. Rev. D* **41**, 83 (1990).
- [19] S. J. Brodsky *et al.*, *Phys. Lett. B* **530**, 99 (2002).
- [20] J. C. Collins, *Phys. Lett. B* **536**, 43 (2002).
- [21] Z. Lu and I. Schmidt, *Phys. Rev. D* **75**, 073008 (2007).
- [22] A. V. Efremov and O. Teryaev, *Sov. J. Nucl. Phys.* **36**, 140 (1982).
- [23] A. Efremov and O. Teryaev, *Phys. Lett. B* **150**, 383 (1985).
- [24] J. Qiu and G. Sterman, *Phys. Rev. Lett.* **67**, 2264 (1991).
- [25] J. Qiu and G. Sterman, *Phys. Rev. D* **59**, 014004 (1998).
- [26] X. Ji, J.-W. Qiu, W. Vogelsang, and F. Yuan, *Phys. Rev. Lett.* **97**, 082002 (2006).
- [27] D. Boer *et al.*, *Nucl. Phys. B* **667**, 201 (2003).
- [28] F. Yuan and J. Zhou, *Phys. Rev. Lett.* **103**, 052001 (2009).
- [29] Z.-B. Kang, J.-W. Qiu, W. Vogelsang, and F. Yuan, *Phys. Rev. D* **83**, 094001 (2011).
- [30] Z.-B. Kang, A. Metz, J.-W. Qiu, and J. Zhou, *Phys. Rev. D* **84**, 034046 (2011).
- [31] M. Anselmino *et al.*, *Eur. Phys. J. C* **13**, 519 (2000).
- [32] Y. Koike, *AIP Conf. Proc.* **675**, 449 (2003).
- [33] Y. Koike, *Nuclear Physics A* **721**, C364 (2003).
- [34] B. Sun *et al.*, *Eur. Phys. J. C* **65**, 163 (2010).
- [35] D. Sivers, *Phys. Rev. D* **43**, 261 (1991).
- [36] K. Allada, Ph.D. thesis, University of Kentucky (2010).
- [37] J. Alcorn *et al.*, *Nucl. Instrum. Meth. A* **522**, 294 (2004).
- [38] F. Bissey, V. Guzey, M. Strikman, and A. Thomas, *Phys. Rev. C* **65**, 064317 (2002).
- [39] E. Babcock, I. A. Nelson, S. Kadlecik, and T. G. Walker, *Phys. Rev. A* **71**, 013414 (2005).
- [40] G. Urciuoli *et al.*, *Nucl. Instrum. Meth. A* **612**, 56 (2009).
- [41] S. Scopetta, *Phys. Rev. D* **75**, 054005 (2007).
- [42] K. Allada, *EPJ Web of Conferences* **37**, 01028 (2012).
- [43] “Jefferson lab experiments,” http://wwwold.jlab.org/exp_prog/12GEV_EXP/, E12-09-018, E12-10-006, E12-11-108, E12-11-111.